# Bond Behavior of Near-Surface Mounted CFRP Laminate Strips under Monotonic and Cyclic Loading

José M. Sena Cruz[1]; Joaquim A. O. Barros[2]; Ravindra Gettu[3]; and Álvaro F. M. Azevedo[4]

**Abstract:** Near-surface mounted (NSM) carbon fiber reinforced polymer (CFRP) laminate strips are used to increase the load-carrying capacity of concrete structures. This is done by inserting the CFRP strips into slits made in the concrete cover of the elements to be strengthened and gluing the strips to the concrete with an epoxy adhesive. In several cases the NSM technique has substantial advantages when compared with externally bonded laminates. To assess the bond behavior between the CFRP and concrete under monotonic and cyclic loading, an experimental program was carried out based on a series of pullout-bending tests. The influence of the bond length and loading history on the bond behavior was investigated. In this work the details of the tests are described and the obtained results discussed. Using the experimental data and an analytical-numerical strategy, a local bond stress-slip relationship was determined. A finite-element analysis was performed to evaluate the influence of the adhesive on the global response observed in the pullout-bending tests.

**DOI:** 10.1061/(ASCE)1090-0268(2006)10:4(295)

**CE Database subject headings:** Bonding; Experimentation; Cyclic loads; Fiber reinforced materials; Concrete; Numerical analysis; Laminates.

## Introduction

The near-surface mounted (NSM) technique using laminate strips of carbon fiber-reinforced polymer (CFRP) has been proposed as a strengthening strategy for increasing the load-carrying capacity of concrete members. The term "near-surface" is used to distinguish this technique from the case where externally bonded fiber-reinforced polymer (FRP) reinforcement (EBR) is utilized. The proposed NSM technique consists of inserting CFRP laminate strips into saw cuts or slits made in the concrete cover of the elements to be strengthened. This concept is not completely new, since it was first used in Europe for the strengthening of reinforced concrete structures in the 1940s. This pioneering technique consisted of placing reinforcing bars in grooves located in the concrete cover, after which the grooves were filled with cement mortar (Asplund 1949).

In the present work, FRP laminates take the place of the rebars and an epoxy adhesive replaces the cement mortar. This "reinvented" technique has been used in some applications and several benefits have been pointed out, such as high levels of strengthening efficacy and, when compared with EBR, a significant decrease of the probability of damage resulting from fire, acts of vandalism, mechanical actions, and effects of aging (Ferreira 2001; Barros and Fortes 2002; Tan et al. 2002; Barros and Dias 2003; Hassan and Rizkalla 2003). Besides, the complete installation time associated with the NSM technique is less than in the case of the EBR technique (Barros and Dias 2003).

Since structural strengthening with the NSM CFRP laminate strips is an emerging technique, bond behavior is an important issue that requires more research. In the current context, bond is the phenomenon that allows transfer of stresses between the concrete and reinforcement during the process of loading the reinforced concrete elements. The bond performance influences the ultimate load-carrying capacity of a reinforced element, as well as some serviceability aspects, such as crack width and crack spacing. In a previous work, the influence of bond length, $L_b$, and concrete strength, $f_{cm}$, on the bond performance has been assessed through pullout-bending tests under monotonic loading on specimens with $L_b$=40, 60, or 80 mm and $f_{cm}$=35, 45, or 70 MPa (Sena-Cruz and Barros 2004a). The test setup used in the experimental program was shown to be adequate for evaluation of the bond performance between CFRP laminate strips and concrete. It was also concluded, from a parametric study, that the peak pullout force, the loaded-end slip, and the bond strength were significantly influenced by the bond length but were independent of the concrete strength.

Bond between reinforcement and concrete is intrinsically a three-dimensional problem that, due to its complexity and for the purpose of developing analytical formulations, is split into two unidimensional or bidimensional problems (FIB 2000). Bond behavior along the reinforcement can be treated as a uniaxial problem and modeled by solving the corresponding differential equation, for which the local bond stress-slip relationship must be known. Several researchers have modeled the longitudinal bond behavior of rebars, assuming that the slip and the bond stress are constant along the bond length. Using this approach, which is acceptable for rebars, empirical equations for the local bond

[1]Assistant Professor, Dept. of Civil Engineering, Univ. of Minho, Campus de Azurém, 4810-058 Guimarães, Portugal (corresponding author). E-mail: jsena@civil.uminho.pt

[2]Associate Professor, Dept. of Civil Engineering, Univ. of Minho, Campus de Azurém, 4810-058 Guimarães, Portugal. E-mail: barros@civil.uminho.pt

[3]Professor, Dept. of Civil Engineering, Indian Institute of Technology Madras, Chennai 600036, India. E-mail:gettu@iitm.ac.in

[4]Assistant Professor, Dept. of Civil Engineering, Univ. of Porto, Rua Dr. Roberto Frias, s/n, 4200-465 Porto, Portugal. E-mail: alvaro@fe.up.pt

Note. Discussion open until January 1, 2007. Separate discussions must be submitted for individual papers. To extend the closing date by one month, a written request must be filed with the ASCE Managing Editor. The manuscript for this paper was submitted for review and possible publication on July 14, 2005; approved on October 6, 2005. This paper is part of the ***Journal of Composites for Construction***, Vol. 10, No. 4, August 1, 2006. ©ASCE, ISSN 1090-0268/2006/4-295–303/$25.00.

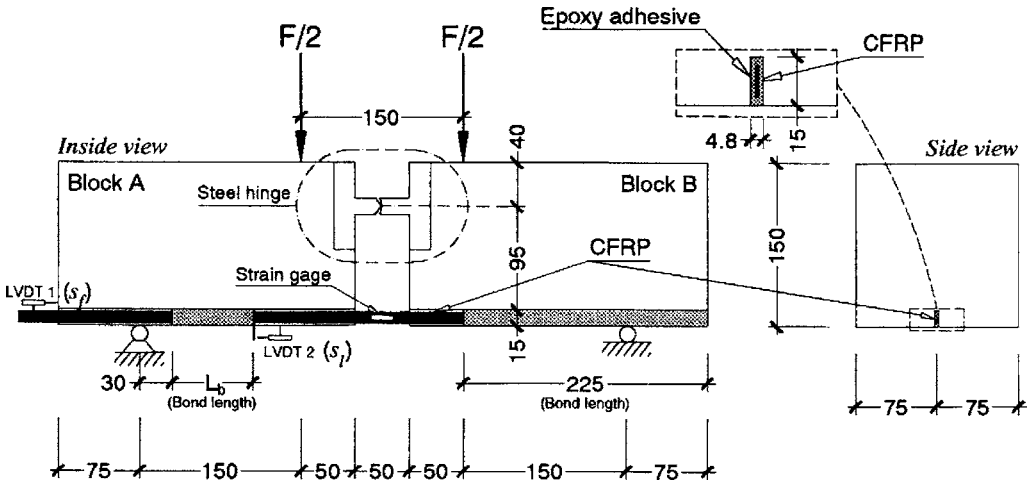


**Fig. 1.** Specimen geometry and test configuration (all dimensions in millimeters)

stress-slip relationship have been proposed [e.g., Eligehausen et al. (1983)].

In early works dealing with analytical modeling of the bond of FRP bars to concrete, the methodology formerly adopted for the rebars was followed. Several researchers have considered a constant slip and bond stress throughout the bond length and, based on this assumption, have proposed different local bond stress-slip relationships for modeling the behavior (Cosenza et al. 1997; De Lorenzis et al. 2002). However, this approach is inaccurate in the case of FRP reinforcement, since the distribution of the slip and bond stress along the bond length is significantly nonlinear (Focacci et al. 2000).

An experimental program was carried out to assess the influence of the bond length and load history on the bond performance of the NSM strengthening technique. These tests are described, and the results obtained are presented and analyzed in the following sections. In accordance with these results, an analytical local bond stress-slip relationship is proposed. The influence of the adhesive on the global response observed in the pullout-bending tests was evaluated through finite-element analysis.

## Experimental Program

### *Specimen and Test Configuration*

Fig. 1 shows the pullout-bending test setup adopted in this study. Concrete blocks A and B are connected by a steel hinge located at midspan close to the top, and by the CFRP laminate fixed at the bottom. The bond test region was located in block A, with the bond length, $L_b$, being one of the variables. To ensure negligible slip of the laminate fixed to block B and to force bond failure in block A, the laminate was bonded over a considerable length in block B. The slit made for the insertion of the CFRP was 15 mm deep and 4.8 mm wide; these dimensions are typical for cuts that can be easily made on site with a rotary saw.

The displacement transducer LVDT2 was used to control the test and also to measure the slip at the loaded end, $s_l$, while the transducer LVDT1 was used to measure the slip at the free end, $s_f$. Note that the loaded-end slip values include the elastic axial deformation of the laminate. A constant 5 μm/s loaded-end slip rate was applied in the tests. This slip rate leads to quasi-static tests where dynamic as well as creep effects are negligible. The strain gauge glued to the CFRP at the midspan of the specimen was used to estimate the pullout force of the laminate. A load cell mounted on the actuator was used to measure the total applied force $F$. The tests were performed in a servohydraulic INSTRON 8505 system of 1 MN capacity with a closed-loop digital controller. Further details on the characteristics of the test setup can be found in Sena-Cruz (2004).

### *Test Procedure*

Suitable bond lengths were adopted to avoid rupture of the CFRP laminate during the test. For this purpose, some preliminary tests were carried out with different bond lengths. Based on these results, the range of 60 to 120 mm was chosen for the bond length. The lower limit of 60 mm was considered to minimize the end effects, and the upper limit of 120 mm was adopted due to limitations associated with the geometry of the specimen.

The influence of the loading history on the bond performance associated with the NSM strengthening technique was treated in the present study by considering the following three types of load configurations: monotonic loading (M), 1 cycle of unloading/reloading at different slip levels (C1), and 10 cycles of unloading/reloading for a fixed load level (C10). The experimental program consists of seven series of tests (Table 1), each consisting of tests on three specimens. The generic denomination of each series is LbX_Y, where $X$ is the CFRP bond length in millimeters (60, 90, or 120 mm) and $Y$ is the type of load configuration (M, C1, or C10).

Three distinct C10 load configurations were adopted: the Lb60_C10, Lb90_C10, and Lb120_C10 series. In these three series, the load level at the onset of the unloading/reloading cycles was 90, 60, and 75% of the peak pullout force, respectively. After the unloading/reloading cycles, the loading was continued monotonically until a 5 mm loaded-end slip measured with LVDT2 (Fig. 2). The objective of the application of unloading/reloading cycles before reaching the maximum pullout force was to assess the influence of the cyclic loading on the bond strength. Cycles were performed at different bond stress levels (60, 75, or 90%) to evaluate the influence of this parameter on the bond stress degradation and on the consequent variation of the bond strength.

In the C1 load configuration (Fig. 3), one unloading/reloading cycle was performed at a slip of 250, 500, 750, 1,000, 1,500, 2,000, 3,000, and 4,000 μm. This load configuration was selected

**Table 1.** Average Values of Parameters Evaluated and Coefficients of Variation (in Parentheses)

| Series | $s_{l\max}$ (mm) | $F_{l\max}$ (kN) | $\tau_{\max}$ (MPa) | $\sigma_{l\max}/f_{fu}$ (%) | $\tau_r/\tau_{\max}$ |
|---|---|---|---|---|---|
| Lb60_M | 0.43 (±11.3%) | 18.7 (±5.1%) | 15.6 | 47.5 | 0.45 (±4.9%) |
| Lb90_M | 0.79 (±9.0%) | 23.9 (±4.1%) | 13.3 | 60.7 | 0.52 (±2.2%) |
| Lb120_M | 1.13 (±8.1%) | 27.7(±2.8%) | 11.5 | 70.5 | 0.54 (±0.9%) |
| Lb60_C10 | 0.35 (±13.4%) | 16.6 (±5.2%) | 13.8 | 42.2 | 0.43 (±3.6%) |
| Lb90_C10 | 0.69 (±12.0%) | 22.2 (±4.7%) | 12.3 | 56.4 | 0.49 (±3.1%) |
| Lb120_C10 | 1.20 (±8.4%) | 28.8 (±4.1%) | 12.0 | 73.2 | 0.56 (±2.6%) |
| Lb120_C1 | 1.18 (±2.8%) | 29.6 (±6.9%) | 12.3 | 75.5 | 0.54 (±1.4%) |

to investigate the influence of cyclic loading on variation of stiffness. Due to some limitations of the testing equipment, all unloading phases were performed under load control with a predetermined load rate that corresponds to an average slip rate of 5 μm/s.

### Material Properties

Concrete designed for a characteristic 28-day cylinder compressive strength of 30 MPa was used in the study. The grain size distributions of the sand and gravel used and the composition of the concrete are given in Sena-Cruz (2004). To avoid shear failure of the concrete blocks, as observed in previous studies (Sena-Cruz et al. 2001), 60 kg/m$^3$ of hooked-end steel fibers were incorporated in the concrete to increase its shear-cracking resistance. Adding fibers to concrete does not affect the bond behavior, since concrete cracking is not expected to occur in the bonding zone (Ezeldin and Balaguru 1989). Cylinder specimens with a diameter of 150 mm and a height of 300 mm were used to obtain the compressive strength of the concrete. The compression tests were carried out in an IBERTEST machine under load control at a rate of 0.5 MPa/s. An average compressive strength of 41.0±0.9 MPa was obtained at the age of the pullout-bending tests (Sena-Cruz 2004).

The CFRP strips used as inserts had a thickness of 1.4 mm and a width of 10.0 mm. The CFRP used is composed of unidirectional carbon fibers in an epoxy matrix, and the strips have a smooth surface. From five uniaxial tensile tests carried out according to ISO 527-5 (ISO 1997) recommendations, the following properties were obtained: Young's modulus of elasticity equal to 171±1 GPa, tensile strength equal to 2.83±0.16 GPa, and ultimate strain equal to 1.55±0.10%.

The laminate was bonded to concrete with a low-viscosity epoxy (Mbrace Epoxikleber 220). To characterize the epoxy, three-point bending and compression tests were carried out, following the NP-EN 196-1 (CEN 1987) recommendations. The epoxy components were mixed in a mortar mixer, placed in the molds, and jolted to ensure adequate filling. The specimens were cured in a curing chamber (20°C and 50% RH). Further details regarding preparation of the epoxy specimens and the corresponding curing procedures can be found elsewhere (Sena-Cruz 2004). The bending tests were carried out in a universal test machine, under load control, at a rate of 50 N/s, and a tensile strength of 21.8±5.5 MPa was obtained from three specimens. In the fracture surface of the specimens, several voids were observed, which can be responsible for the large coefficient of variation (i.e., 25%). After completing the bending tests, the half-beams were tested in compression. These tests were performed in a universal testing machine, under load control, at a rate of 2.4 kN/s, and a compressive strength of 67.5±3.6 MPa was obtained from six epoxy specimens.

### Specimen Preparation

The blocks that comprise the pullout-bending specimens were cured in a fog room for 28 days after casting. A table-mounted

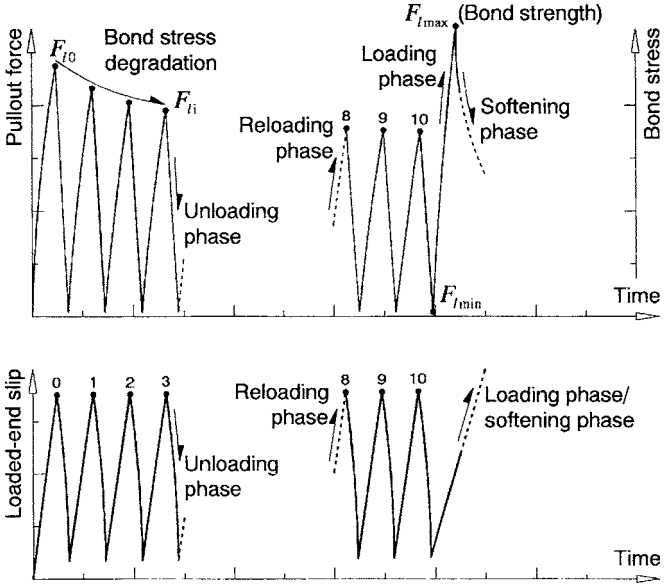


**Fig. 2.** Loading scheme of C10 cyclic tests

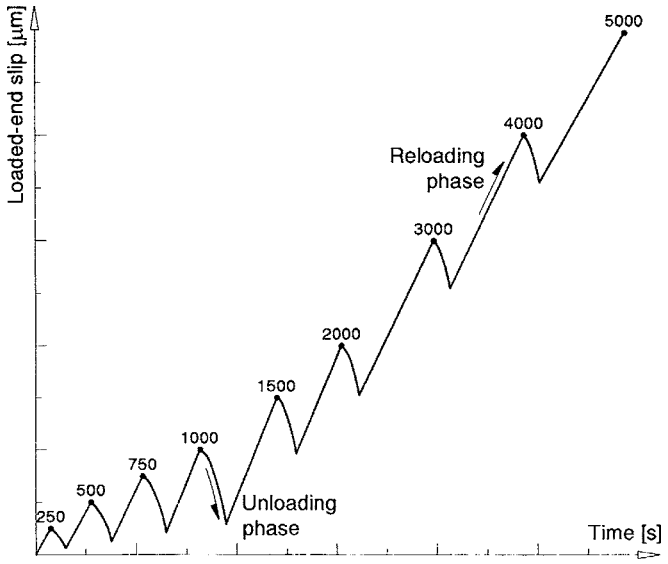


**Fig. 3.** Loading scheme of C1 cyclic tests

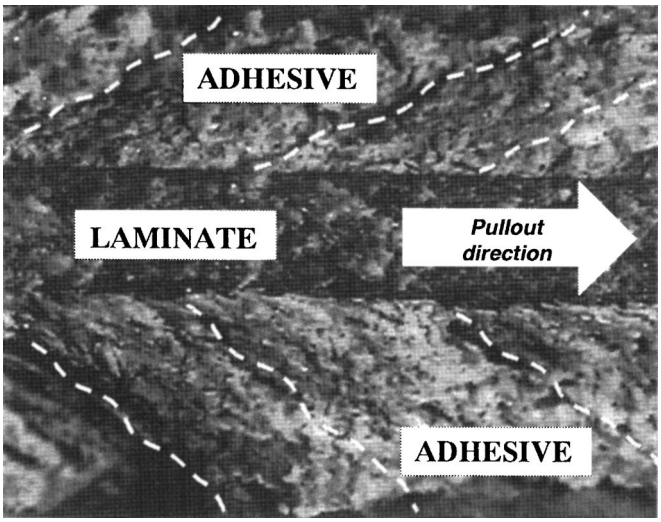


**Fig. 4.** Crack pattern observed in laminate-adhesive-concrete bonding zone

saw was used to open the slits, which then were cleaned with compressed water to eliminate the remaining dust induced by the sawing process. Afterward, the specimens were air-dried in the laboratory environment during at least 1 week before the CFRP laminates were bonded. Immediately before bonding the CFRP laminate, the slits were cleaned with a jet of compressed air. To avoid the flow of epoxy adhesive beyond the bond length, a masking procedure was adopted (Sena-Cruz 2004).

Preparation of the CFRP strip involved the following steps: delimiting the bond length carefully, gluing a strain gauge at mid-span, and, finally, cleaning the CFRP with acetone (Sena-Cruz 2004).

In the bond regions the slit was completely filled with epoxy adhesive. In the corresponding lateral surfaces the laminate was covered with a thin layer of epoxy adhesive. Afterward, the laminate was inserted forcibly into the slit, resulting in the flow of excess adhesive out of the slit. Finally, the overflowed epoxy adhesive was removed and the surface leveled, and the specimens were kept for several weeks in the laboratory environment before being tested.

## Results

In all the tested specimens, slip was mainly localized along the CFRP-adhesive interface. This was to be expected since the rougher surface of the concrete leads to better bonding with the adhesive, resulting in much more slip at the laminate-adhesive interface during failure than along the concrete-adhesive interface. Additionally, fine cracks in a fishbone pattern were observed in the epoxy adhesive (Fig. 4). No cracks were observed on the concrete surface, justifying the assumption that the concrete tensile strength and the addition of fibers to the concrete play a negligible role in the behavior observed in the present tests.

### *Monotonic Results*

Fig. 5 shows typical relationships between the pullout force and the slip, at both the free end and loaded end ($F_l$–$s_f$ and $F_l$–$s_l$), for the monotonic load configuration. Complete details related to

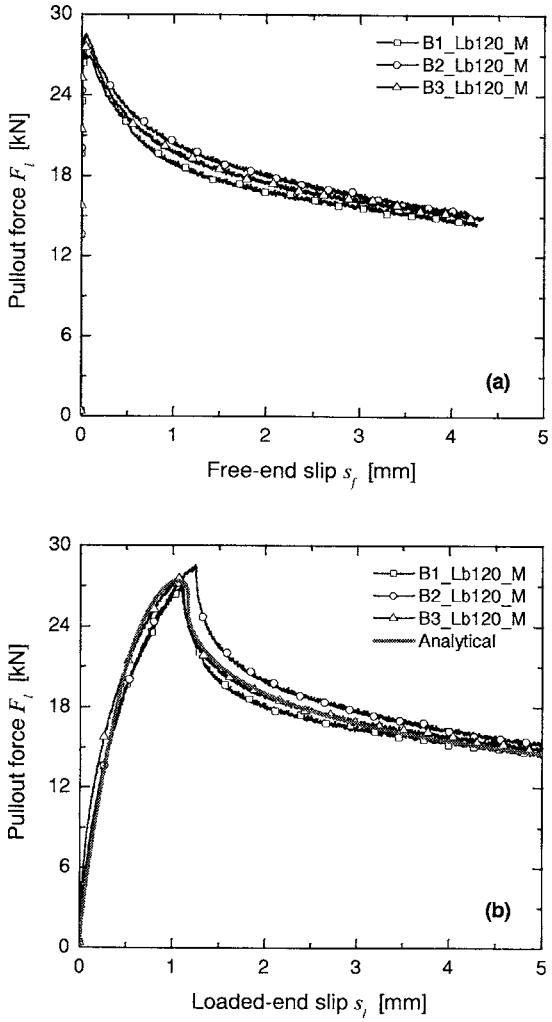


**Fig. 5.** Variation of pullout force with (a) free-end slip; (b) loaded-end slip for Lb120_M series

monotonic loading can be found in Sena-Cruz (2004). In the present work, the loaded-end slip includes the axial deformation of the laminate. Calculation of the pullout force in the CFRP, $F_l$, was based on the strains recorded by the gauges mounted on the CFRP laminate, considering a modulus of elasticity of 171 GPa and a cross-sectional area of 14.04 mm$^2$. Fig. 5 shows the nonlinear relationship between the slip and the pullout force. For all the monotonic tests, peak loads occurred at loaded-end slips ranging from 0.27 to 1.24 mm. After a sharp postpeak drop, the pullout force slowly decreases with an increase in the slip. The residual pullout forces, which are significant, indicate that frictional mechanisms in the laminate-adhesive-concrete interfaces are mobilized during the pullout failure.

To assess the bond performance under monotonic loading, the following parameters have been analyzed (Table 1):

- $s_{l\,\max}$=slip at loaded end at peak pullout force ($F_{l\,\max}$);
- $\tau_{\max}$=average bond strength, obtained by dividing peak pullout force by contact area between CFRP and epoxy adhesive, $F_{l\,\max}/(2w_fL_b)$, where $w_f$ is width of laminate;
- $\sigma_{l\,\max}/f_{fu}$=ratio between axial stress in laminate at peak pullout force and its tensile strength; and

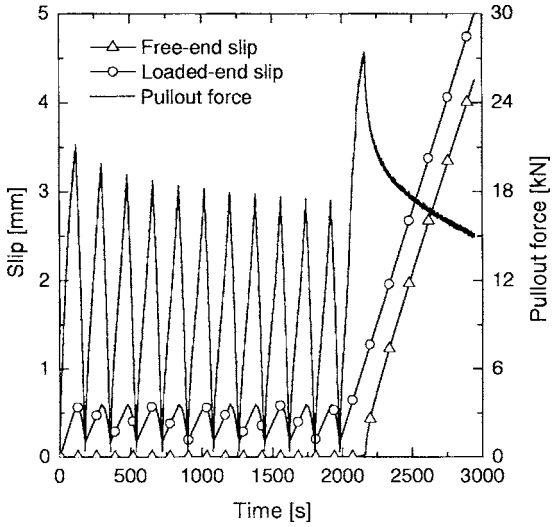


**Fig. 6.** Evolution of slip at free end and loaded end and of pullout force of first specimen of Lb120_C10 series

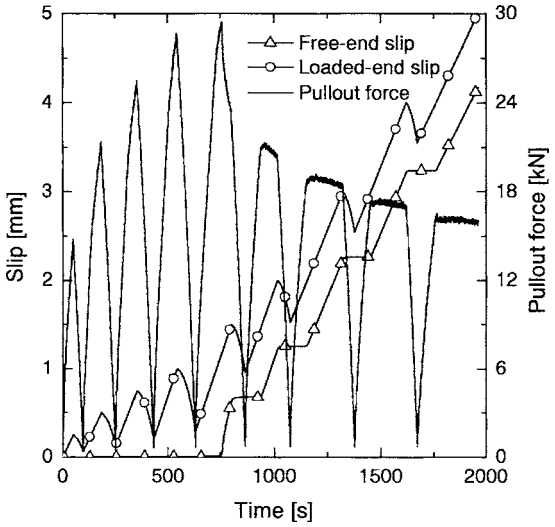


**Fig. 7.** Evolution of slip at free end and loaded end and of pullout force of first specimen of Lb120_C1 series

- $\tau_r/\tau_{max}$=residual bond stress ratio, where $\tau_r$=average bond stress at end of test, which corresponds to 5 mm loaded-end slip.

As expected, the parameters $s_{l\,max}, F_{l\,max}, \sigma_{l\,max}/f_{fu}$, and $\tau_r/\tau_{max}$ increase with bond length, $L_b$. The average peak bond stress, $\tau_{max}$, however, decreases with $L_b$.

### *Cyclic Loading Results*

Fig. 6 presents, for the C10 series, the typical evolutions of the slip at the free end and the loaded end, and of the pullout force. As this figure shows, the free-end slip is negligible during the unloading/reloading cycles, indicating that the bond failure has not progressed through the bonded length. The loaded-end slip has a nonlinear evolution with time during unloading since the tests were performed under load control in each unloading phase. Note that to guarantee the stability of the test, unloading was stopped at about 0.5 kN (instead of going down to zero load). It can be observed that the maximum pullout force reached at the end of reloading, during the cycles, decreases progressively, indicating some degradation of the bond due to the loading applied. In the posterior monotonic loading phase of the tests, both the free-end and loaded-end slips evolve with a similar slope, and the pullout force reaches a peak value after which it progressively decreases.

Fig. 7 illustrates the typical evolutions of the slip at the free end and loaded end, and of the pullout force for the C1 series. Until the peak pullout force is reached, there is practically no free-end slip, with some of the loaded-end slip being recovered during the unloading phase. After the peak pullout force, both the free-end and loaded-end slips increase during the loading phase, while in the unloading phase the free-end slip remains constant, whereas the loaded-end slip decreases. This trend can be explained by assuming that the degradation of the interface spreads over the complete bond length at the peak pullout force, and any further pullout increases the degradation leading to a decrease in the pullout resistance. Nevertheless, the frictional restraint continues to be significant even after a slip of 5 mm.

Fig. 8 shows the typical relationship between the pullout force and the slip at the free end and loaded end ($F_l$–$s_f$ and $F_l$–$s_l$) for the C10 series. The complete test data for this series can be found in Sena-Cruz (2004), and the corresponding monotonic curve (Lb120_M) is included in Fig. 8. This curve is the average response of the specimens having the same bond length. The curves of the C10 series are similar in shape to that of the corresponding monotonic test. In the series with bond lengths of 60 and 90 mm the monotonic curve is an upper bound of the cyclic test results, whereas in the series with a bond length of 120 mm the monotonic curve is a lower bound (Sena-Cruz 2004).

Fig. 9 illustrates the typical relationship between the loaded-end slip and the pullout force for the cyclic loading phase of the C10 series. In the first cycle (thick line in Fig. 9), a distinct behavior can be observed: in the unloading branch, the relationship is nonlinear with upward concavity, and in the initial part of the reloading branch the behavior is nonlinear followed by a linear relationship up to the end of this branch. In subsequent cycles, there is no linear part in the reloading branch.

For the C1 series, the relationships between the pullout force and the slip at the free and loaded ends ($F_l$–$s_f$ and $F_l$–$s_l$) are shown in Fig. 10, along with the corresponding monotonic curve. As expected, the curves of the cyclic tests have a shape similar to the monotonic curve. As in the case of the Lb120_C10 series, the monotonic curve is close to the lower bound of the corresponding cyclic test results. Also, the free-end slip remains constant during the unloading and reloading phases, indicating that the bond has not degraded along all its length.

Table 1 presents the values of the parameters derived from the experimental results, as defined in the previous section. In general, the values obtained in cyclic tests are lower than the corresponding results of the monotonic tests with the exception of series Lb120. As seen earlier, the parameters $s_{l\max}, F_{l\max}, \sigma_{l\max}/f_{fu}$ and $\tau_r/\tau_{max}$ tend to increase with the bond length, $L_b$, whereas $\tau_{max}$ decreases with an increase in $L_b$.

For the C10 series, the influence of the number of cycles on the normalized pullout force has been represented in Fig. 11(a). For each test, $F_{li}$ is the pullout force at the end of the $i$th reloading branch (Fig. 2). The influence of the cyclic loading on the strength degradation was similar in all series with an average strength reduction of about 17%. A more significant degradation occurred in the B3_Lb60_C10 specimen, after the fifth cycle, since all the cycles were performed in the postpeak regime. In the remaining specimens, all the cycles were carried out before the

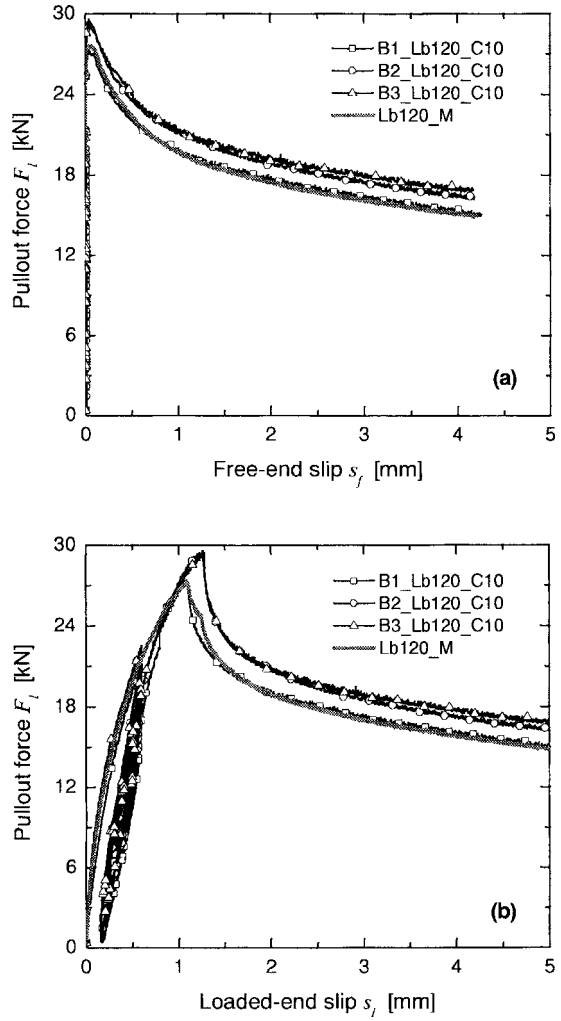


**Fig. 8.** Variation of pullout force with (a) free-end slip; (b) loaded-end slip for Lb120_C10 series

peak load was reached. Note that due to the inherent variability between the specimens, the cycles did not begin exactly at the desired ratio between $F_{l0}$ and $F_{l\,\max}$ (i.e., 60% for Lb90 series, 75% for Lb120 series, and 90% for Lb60 series) since the value of $F_{l0}$ was obtained from the monotonic tests.

Fig. 11(b) represents the stiffness degradation in the C1 series. This stiffness has been defined as the slope of the line connecting the points corresponding to the beginning of the unloading and reloading phases. Note that up to the peak pullout force, the stiffness decreases significantly, followed by a slight increase in the first part of the softening branch and then a slight decrease. This trend can be attributed to the progressive debonding of the CFRP-adhesive and adhesive-concrete interfaces up to the peak pullout force, along with adhesive cracking. Later, in the postpeak regime, the sudden decay of the pullout force induces the typical increase of stiffness that occurs when materials are submitted to large instantaneous load or displacement variations, as reported by Otter and Naaman (1986). When this phenomenon stabilizes, the bond stiffness is governed by friction between the slipping surfaces and decreases slightly as the slip increases.

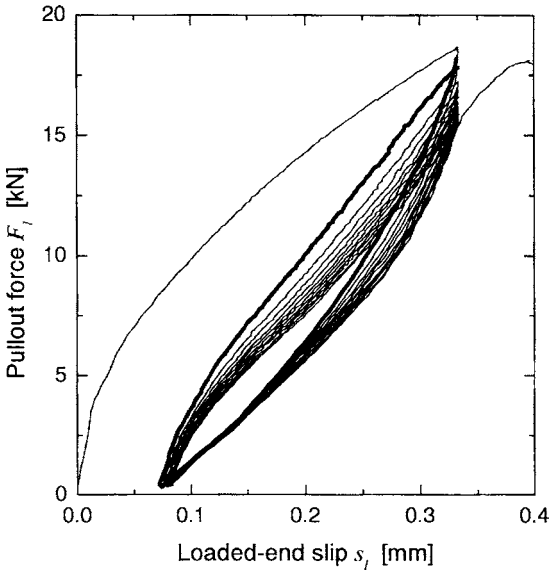


**Fig. 9.** Curves of pullout force versus loaded-end slip of B1_Lb60_C10 specimen during all cycles

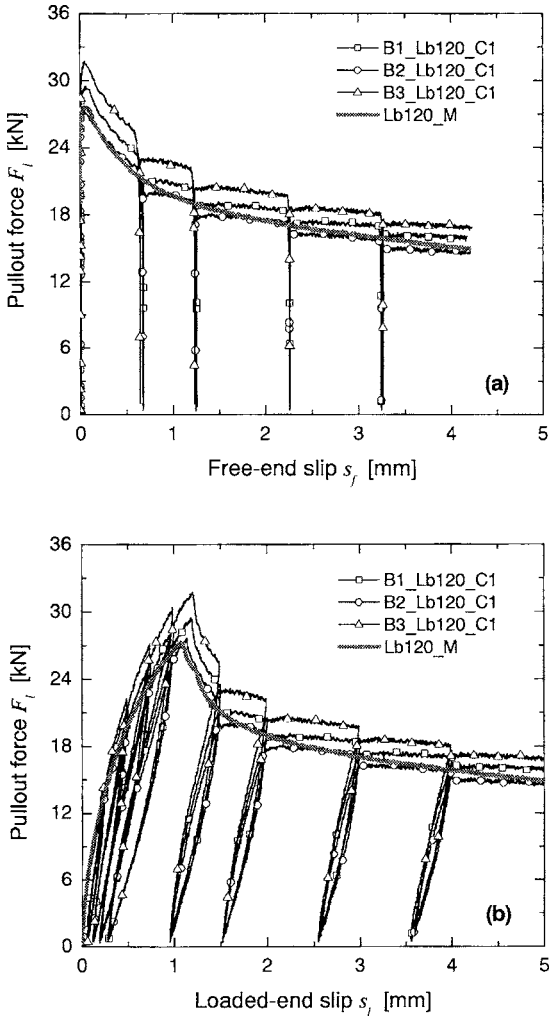


**Fig. 10.** Variation of pullout force with (a) free-end slip; (b) loaded-end slip for Lb120_C1 series

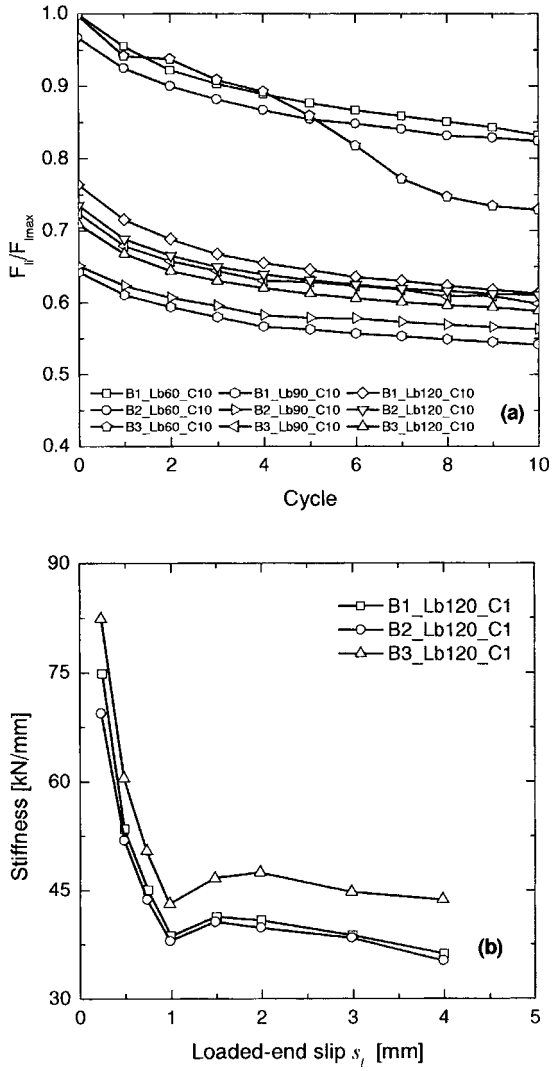


**Fig. 11.** (a) Normalized pullout force as function of number of cycles; (b) stiffness degradation in Lb120_C1 series

## Bond Modeling

### *Analytical Modeling*

The following differential equation can be taken to govern the slip of the laminate bonded to concrete, as shown by Sena-Cruz and Barros (2004b)

$$\frac{d^2s}{dx^2} = \frac{2}{t_f E_f}\tau \tag{1}$$

where $t_f$ and $E_f$=thickness and Young's modulus of the CFRP laminate, respectively; $s$=slip, i.e., the relative displacement between the laminate and concrete; $\tau=\tau(s)$=local bond stress-slip relationship within the length $dx$; and $\tau$=bond stress in the laminate-adhesive interface. Eq. (1) is only valid when the following assumptions hold:

- CFRP laminate exhibits linear-elastic behavior in longitudinal direction; and
- Deformation of concrete and adhesive is neglected, along with slip in adhesive-concrete interface.

In the present work, the local bond stress-slip relationship is defined by the following functions:

$$\tau(s) = \tau_m\left(\frac{s}{s_m}\right)^{\alpha}, \quad \text{if } s \le s_m \tag{2}$$

$$\tau(s) = \tau_m\frac{1}{1+\left(\frac{s-s_m}{s_1}\right)^{\alpha'}}, \quad \text{if } s > s_m \tag{3}$$

In these equations, $\tau_m$ and $s_m$ are the bond strength and the corresponding slip, respectively, and $\alpha$, $\alpha'$, and $s_1$ are the parameters that define the shape of the corresponding curve. For the current values of $\alpha$ ($0<\alpha<1$), it can be verified that the initial slope of the line defined by Eq. (2) is equal to infinity, thus leading to a reasonable approximation of the bond stress-slip phenomenon. In fact, the experimental tests carried out in the present work [e.g., see data in Fig. 5] have shown that the slip is negligible for small values of the bond stress.

A numerical strategy was developed (Sena-Cruz and Barros 2004b) using the loaded-end slip and the pullout force values obtained in the pullout-bending tests described in the previous section. This approach yields the values of the parameters $s_m$, $\tau_m$, $\alpha$, $\alpha'$, and $s_1$ of Eqs. (2) and (3) by solving Eq. (1). The distribution of the slip and the bond stress along the bond length is taken into account. Fig. 5(b) shows, for one of the tests in the monotonic series, that the analytically obtained pullout force versus loaded-end slip relationship fits the corresponding experimental results satisfactorily. Similar results have been obtained for the other monotonic series (Sena-Cruz 2004).

The values of the parameters that define the $\tau(s)$ relationship and the values of the normalized errors obtained in each analysis are presented in Table 2. The normalized error, $\bar{e}$, is the ratio between $e$ and the area under the experimental curve, where $e$ is the area between the experimental and numerical curves. For each series (composed of three specimens), the experimental curve is the average relationship between the loaded-end slip and the pullout force. Based on the results given in Table 2, the following observations can be made:

- Normalized errors in all series are acceptable;
- As expected, $s_m$ increases with bond length, since adhesive deformation is neglected in present approach;
- Decrease of $\tau_m$ with the increase of bond length can be

**Table 2.** Values of Parameters Defining Local Bond Stress-Slip Relationship

| Series | $s_m$ (mm) | $s_1$ (mm) | $\tau_m$ (MPa) | $\alpha$ | $\alpha'$ | $\bar{e}$ (%) |
|---|---|---|---|---|---|---|
| Lb60_M | 0.26 | 1.8 | 17.5 | 0.40 | 0.40 | 1.2 |
| Lb90_M | 0.45 | 2.0 | 15.7 | 0.45 | 0.35 | 1.6 |
| Lb120_M | 0.47 | 2.0 | 14.3 | 0.50 | 0.41 | 2.5 |
| Average | 0.39 (±29.5%) | 1.9 (±6.0%) | 15.8 (±10.1%) | 0.45 (±11.1%) | 0.39 (±8.3%) | — |

Note: Values in parentheses are coefficients of variation of corresponding series.

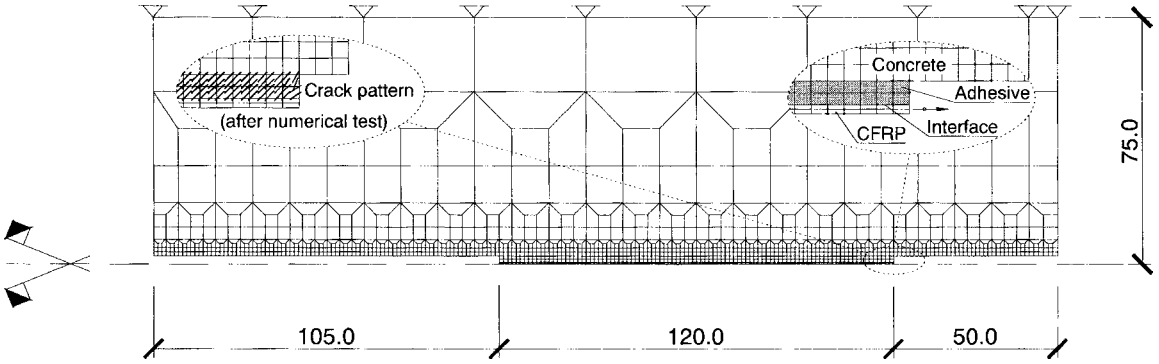


**Fig. 12.** Finite model: geometry, mesh, loading configuration, support conditions, and crack pattern (all dimensions are in millimeters)

observed. The coefficient of variation of the bond strength is small; and
- Small coefficients of variation were obtained for $s'$, $\alpha$, and $\alpha'$.

### *Numerical Modeling*

Several numerical analyses were performed to evaluate the influence of the adhesive on the global response of the pullout-bending tests. The horizontal cross-section, at laminate level, of the pullout-bending test was modeled as a plane stress problem. Fig. 12 shows the finite-element model used in simulation of the beams with 120 mm bond length. In this model, four-node Lagrangian plane stress elements with a $2\times2$ Gauss-Legendre integration scheme were used to simulate the concrete beam, as well as the adhesive and the CFRP laminate. The bond between the laminate and adhesive was simulated by four-node line interface elements with a two-point Lobatto integration rule. Perfect bond was considered along the adhesive-concrete interface. The concrete and adhesive zones were taken to be 15 mm thick, whereas the thickness of the CFRP laminate and the CFRP-adhesive interface zone was 10 mm. The concrete and CFRP materials were modeled as linear elastic, considering the moduli of elasticity of 34.4 and 171 GPa, and Poisson's ratios of 0.2 and 0.0, respectively.

Assuming that the normal stiffness of the interface element has a marginal effect on the bond behavior, a constant value of $10^6$ N/mm$^3$ was adopted. According to Schellekens (1992), a value with this order of magnitude is required to avoid numerical instabilities. The values of the parameters used to define the tangential behavior of the interface elements [$\tau(s)$ relationship] are given in Table 2. A multifixed smeared crack model was used to simulate the brittle behavior of the epoxy adhesive (Sena-Cruz 2004). A Young's modulus of 7 GPa, a Poisson's ratio of 0.25, and a tensile strength of 7.0 MPa were adopted for the epoxy adhesive. The load was applied at the loaded end of the laminate by direct displacement control. All the analyses were performed using the FEMIX computer code, which is a general-purpose finite-element program (Azevedo et al. 2003).

The results of the numerical analyses practically coincide with the results obtained analytically. Observe that the numerically obtained global response was not affected by the deformation of the adhesive. Fig. 12 also shows the crack pattern obtained numerically for the case of the beam Lb120_M. This crack pattern is similar to that observed in the experiments (Fig. 4).

## Conclusions

The bond performance of the near-surface-mounted CFRP laminate strips was assessed by means of pullout-bending tests under monotonic and cyclic loading. The influence of the bond length, $L_b$ and of the load history were analyzed by carrying out a series of tests with $L_b$=60, 90, or 120 mm, under monotonic and cyclic loadings.

Based on the results obtained in the monotonic tests, the following conclusions can be made: the peak pullout force increases with $L_b$; the average bond strength ranges from 10 to 14 MPa, with a tendency to decrease when $L_b$ increases; and the maximum tensile stress in the CFRP laminate and the loaded-end slip at peak pullout force increase with $L_b$.

The results of the unloading/reloading tests with a fixed-load level lead to the following conclusions: the pullout force versus slip relationships in the cyclic tests and the curve obtained in the corresponding monotonic tests have a similar shape; in the unloading/reloading cycles a decrease of the pullout force at the end of the reloading branches, carried out before the peak pullout force, was observed; and the peak pullout force was not influenced by the cyclic loading. In the unloading/reloading tests at different slip levels, the stiffness decreases significantly up to the peak pullout force, after which there is a slight increase followed by a smooth decrease.

Using a numerical approach, a local bond stress-slip relationship was obtained from the test results. The parameters that define this relationship were, however, found to be dependent on the bond length. Finite-element analysis was performed with the aim of evaluating the influence of the epoxy adhesive on the global response, and it was found to be negligible. The crack pattern obtained numerically matches the experimental observations.

## Acknowledgments

The first writer wishes to acknowledge the grant SFRH/BD/3259/2000 provided by FCT (Portuguese Foundation for Science and Technology) and FSE (European Social Fund). The tests were performed at the Structural Technology Laboratory of the Technical University of Catalonia, Spain, with the help of Miguel Angel Martín and Ernesto Diaz. The writers wish to acknowledge the support provided by S&P and Bettor MBT, who supplied the material used in the study.

## Notation

*The following symbols are used in this paper*:

$e$ = area between experimental and numerical curves;
$\bar{e}$ = ratio between $e$ and area beneath experimental curve;
$F_l$ = pullout force at loaded end of laminate;
$F_{l\,\max}$ = peak pullout force at loaded end of laminate;
$f_{cm}$ = concrete compressive strength;
$f_{fu}$ = laminate tensile strength;
$L_b$ = bond length;
$s_f$ = free-end slip;
$s_l$ = loaded-end slip;
$s_{l\,\max}$ = loaded-end slip at peak pullout force;
$s_m$ = slip at peak bond stress (local bond stress-slip relationship);
$t_f$ = laminate thickness;
$w_f$ = laminate width;
$\alpha$ = parameter used in definition of local bond stress-slip relationship;
$\alpha'$ = parameter used in definition of local bond stress-slip relationship;
$\sigma_{l\,\max}$ = axial stress at peak pullout force at loaded end of laminate;
$\tau_{\max}$ = average bond strength;
$\tau_m$ = bond strength (local bond stress-slip relationship); and
$\tau_r$ = average bond stress at end of test.

## References


Asplund, S. O. (1949). "Strengthening bridge slabs with grouted reinforcement." *ACI J.*, 20(6), 397–406.

Azevedo, A. F. M., Barros, J. A. O., Sena-Cruz, J. M., and Gouveia, A. V. (2003). "Software no ensino e no projecto de estruturas. Educational software for the design of structures." *Proc., III Congresso de Luso-Moçambicano de Engenharia*, J. S. Gomes, C. F. Afonso, C. C. António, and A. S. Matos, eds., Maputo, Mozambique, 81–92 (in Portuguese).

Barros, J. A. O., and Dias, S. J. E. (2003). "Shear strengthening of reinforced concrete beams with laminate strips of CFRP." *Proc., Int. Conf. of Composites in Construction*, D. Bruno, G. Spadea, and N. Swamy, eds., Cosenza, Italy, 289–294, ⟨http://www.civil.uminho.pt/composites⟩ (July 4, 2005).

Barros, J. A. O., and Fortes, A. S. (2002). "Concrete beams reinforced with carbon laminates bonded into slits." *Proc., 5th Congreso de Métodos Numéricos en Ingeniería* (CD-ROM), Madrid, ⟨http://www.civil.uminho.pt/composites⟩ (July 4, 2005).

Cosenza, E., Manfredi, G., and Realfonzo, R. (1997). "Behavior and modeling of bond of FRP rebars to concrete." *J. Compos. Constr.*, 1(2), 40–51.

De Lorenzis, L., Rizzo, A., and La Tegola, A. (2002). "A modified pull-out test for bond of near-surface mounted FRP rods in concrete." *J. Compos. Part B: Eng.*, 33(8), 589–603.

Eligehausen, R., Popov, E. P., and Bertero, V. V. (1983). "Local bond stress-slip relationships of deformed bars under generalized excitations." *Rep. UCB/EERC-83/23*, Earthquake Engineering Research Center, Univ. of California at Berkeley, Berkeley, Calif.

European Committee for Standardization (CEN). (1987). "Methods testing cements." *NP-EN 196-1*, CEN, Brussels.

Ezeldin, A., and Balaguru, P. (1989). "Bond behavior of normal and high strength fiber reinforced concrete." *ACI Mater. J.*, 86, 515–524.

Ferreira, D. R. S. M. (2001). "Pilares de betão armado reforçados com laminados de fibras de carbono. Reinforced concrete columns strengthened with CFRP laminate strips." MSc thesis, Civil Engineering Dept., Univ. of Minho, Portugal, ⟨http://www.civil.uminho.pt/composites (July 4, 2005) (in Portuguese).

International Federation for Structural Concrete (FIB). (2000) "Bond of reinforcement in concrete." *State-of-the-Art Rep. Prepared by Task Group Bond Models: Bulletin No. 10*, FIB, Lausanne, Switzerland.

Focacci, F., Nanni, A., and Bakis, C. E. (2000). "Local bond-slip relationship for FRP reinforcement in concrete." *J. Compos. Constr.*, 4(1), 24–31.

Hassan, T., and Rizkalla, S. (2003). "Investigation of bond in concrete structures strengthened with near surface mounted carbon fiber reinforced polymer strips." *J. Compos. Constr.*, 7(3), 248–257.

International Organization for Standardization (ISO). (1997). "Plastics—Determination of tensile properties. 5: Test conditions for unidirectional fiber-reinforced plastic composites." *ISO 527-5*, ISO, Geneva.

Otter, D., and Naaman, A. E. (1986). "Steel fiber reinforced concrete under static and cyclic compressive loading." *Proc., RILEM Symp. on Developments in Fiber Reinforced Cement and Concrete. 1*, Sheffield, U.K.

Schellekens, J. C. J. (1992). "Computational strategies for composite structures." Ph.D. thesis, Delft Univ. of Technology, Delft, The Netherlands.

Sena-Cruz, J. M. (2004). "Strengthening of concrete structures with near-surface mounted CFRP laminate strips." Ph.D. thesis, Dept. of Civil Engineering, Univ. of Minho, ⟨http://www.civil.uminho.pt/composites⟩ (July 4, 2005).

Sena-Cruz, J. M., and Barros, J. A. O. (2004a). "Bond between near-surface mounted CFRP laminate strips and concrete." *J. Compos. Constr.*, 8(6), 519–527.

Sena-Cruz, J. M., and Barros, J. A. O. (2004b). "Modeling of bond between near-surface mounted CFRP laminate strips and concrete." *Computers and Structures, Special issue: Computational Mechanics*, C. Mota Soares and J. Barbosa, eds., 82/17–19, 1513–1521 (in Portugal).

Sena-Cruz, J. M. S., Barros, J. A. O., and Faria, R. M. C. M. (2001). "Assessing the embedded length of epoxy bonded carbon laminates by pull-out bending tests." *Proc., Int. Conf. on Composites in Construction*, J. Figueiras, L. Juvandes, and R. Faria, eds., Porto, Portugal, 217–222, ⟨http://www.civil.uminho.pt/composites⟩ (July 4, 2005).

Tan, K., Tumialan, G., and Nanni, A. (2002). "Evaluation of CFRP systems for the strengthening of RC slabs." *Rep. CIES 02-38*, Center for Infrastructure Engineering Studies, Univ. of Missouri-Rolla, Rolla, Mo.